Acta Crystallographica Section B
Structural Science
ISSN 0108-7681

Crystal growth and twinned crystal structure of Sr_2CaWO_6

G. Madariaga,[a]* A. Faik,[b] T. Breczewski[b] and J. M. Igartua[b]

[a]Departamento de Física de la Materia Condensada, Facultad de Ciencia y Tecnología, Universidad del País Vasco, Apdo 644, 48080 Bilbao, Spain, and [b]Fisika Aplikatua II Saila, Zientzia eta Teknologia Fakultatea, Euskal Herriko Unibertsitatea, PO Box 644, Bilbao 48080, Spain

Correspondence e-mail: gotzon.madariaga@ehu.es

Received 24 July 2009
Accepted 15 January 2010

Single crystals of Sr_2CaWO_6 have been prepared by sintering at high temperature. Powder samples were compressed into rods and heated up to 1953 K. This seems a promising new route for further studies of the structure and physical properties of double perovskites. The structural model of Sr_2CaWO_6 includes a quantitative description of the twinning shown by the diffraction pattern that should be present in almost any single-crystal specimen for this type of compound.

1. Introduction

During the last few years transition-metal oxide materials with rock-salt ordered perovskite structure ($A_2BB'O_6$) have been extensively studied owing to their wide compositional flexibility that enables them to accommodate almost every element of the periodic table showing a great variety of structures. These metal oxide materials present interesting magnetic and electric properties such as colossal magnetoresistance (Sr_2FeMoO_6; Kobayashi *et al.*, 1998) or superconductivity ($Sr_2YRu_{0.95}Cu_{0.05}O_6$; DeMarco *et al.*, 2000) and they are firm candidates to show multiferroicity. Nevertheless, the lack of samples showing a good crystallization grade and a low level of impurities makes double perovskites more difficult to study. Most of the structural information has been obtained from powder diffraction data (either conventional X-rays or neutrons) and little attention has been paid to the structural transformations occurring in such materials.

Only recently have the structural properties of double perovskites been analyzed systematically. Unfortunately the structural studies of these materials usually combine a low sensitivity of X-rays to the positions of the O atoms (masked by the presence of heavy cations) with high pseudosymmetry, strong absorption for X-rays, and (in some cases) disorder of *B* cations and/or oxygen deficiency. An additional difficulty for the accurate structural determination and the study of their physical properties lies in the fact that single crystals of these compounds have rarely been grown, until the last few years[1] (see Table 1) when a research group has focused on the single-crystal growth of lanthanide (Davis *et al.*, 2004; Gemmill, Smith & zur Loye, 2004; Gemmill *et al.*, 2005; Mugavero, Smith & zur Loye, 2005; Stitzer, Smith & zur Loye, 2002; Mugavero III *et al.*, 2003), tantalum (Roof *et al.*, 2008) and rhenium (Bharathy & zur Loye, 2008) oxides in an effort to investigate both the structural chemistry and the magnetic properties of such compounds. These authors have developed an effective synthetic approach employing molten hydroxide fluxes.

[1] An isolated and interesting exception is the study of the incommensurate structure of Pb_2CoWO_6 at room temperature (Bonin *et al.*, 1995).

Table 1
Listing of double perovskites for which single crystals have been grown, including the preparation method and the space group (superspace group in the case of the incommensurate perovskite Pb_2CoWO_6) at room temperature.

Compound	Method of preparation	Symmetry	Reference
La_2NaIrO_6	'Acidic' high-temperature hydroxide melts	$P2_1/n$	Davis *et al.* (2004)
Pr_2NaIrO_6		$P2_1/n$	
Nd_2NaIrO_6		$P2_1/n$	
La_2NaRuO_6	'Acidic' molten NaOH	$P2_1/n$	Gemmill, Smith & zur Loye (2004)
Pr_2NaRuO_6		$P2_1/n$	
Nd_2NaRuO_6		$P2_1/n$	
La_2NaOsO_6	'Acidic' molten NaOH	$P2_1/n$	Gemmill *et al.* (2005)
Pr_2NaOsO_6		$P2_1/n$	
Nd_2NaOsO_6		$P2_1/n$	
La_2NaTaO_6	High-temperature hydroxide melts	$P2_1/n$	Roof, Smith & Loye (2008)
La_2LiIrO_6	Molten LiOH/KOH fluxes	$P2_1/n$	Mugavero, Smith & zur Loye (2005)
Pr_2LiIrO_6		$P2_1/n$	
Nd_2LiIrO_6		$P2_1/n$	
Sm_2LiIrO_6		$P2_1/n$	
Eu_2LiIrO_6		$P2_1/n$	
Ba_2LiOsO_6	Molten hydroxide flux	$Fm\bar{3}m$	Stitzer *et al.* (2002)
Ba_2NaOsO_6		$Fm\bar{3}m$	
Ba_2LiReO_6	Molten hydroxide flux	$Fm\bar{3}m$	Bharathy & zur Loye (2008)
Ba_2NaReO_6		$Fm\bar{3}m$	
Sr_2LiReO_6		$Fm\bar{3}m$	
Sr_2NaReO_6		$P2_1/n$	
Sm_2NaIrO_6	'Acidic' high-temperature hydroxide melts	$P2_1/n$	Mugavero III *et al.* (2003)
Pb_2CoWO_6	Molten PbO flux	$I2/m(\alpha 0\gamma)0s$	Bonin *et al.* (1995)

However, owing to the difficulties expressed above the use of single crystals does not make the space-group assignation and/or the structure resolution straightforward. Moreover, the latent presence of the cubic perovskite structure may provoke the appearance of ferroelastic twin domains (Bonin *et al.*, 1995) even in samples of size suitable for single-crystal diffraction. As a consequence, in some cases, the symmetry of the proposed structure could be overestimated or misassigned as frequently occurs when powder diffraction is used.

The ideal double perovskite structure of the general formula $A_2BB'O_6$ is obtained when the B cation of the simple perovskite (ABO_3) is substituted by a B' cation in an ordered 1:1 way. Thus, the double perovskite structure ($A_2BB'O_6$) can be represented as a three-dimensional network of alternating BO_6 and $B'O_6$ octahedra, with A cations occupying the 12-coordinated interstitial spaces between the octahedra. This arrangement determines the crystal system and, together with the composition, the physical properties. The aristotype structure of the double perovskites is cubic (Mitchell, 2001) with the space group $Fm\bar{3}m$; however, due to a mismatch between the size of the A-site cation and the cuboctahedral space between the octahedra, many such materials show a cubic distorted room-temperature structure (see Table 1) and undergo one (Chmaissem *et al.*, 2000), two (Yamamura *et al.*, 2006) or even more (Martin *et al.*, 2004) structural phase transitions at different temperatures. These structural transformations can be conveniently described as changes in the way BO_6 and $B'O_6$ are rotated with respect to the crystallographic axes of the material to accommodate the size of the A-site cations (Mitchell, 2001). The space group $P2_1/n$ is rather common at room temperature (see Table 1) given it allows for a fully ordered arrangement of the B and B' cations and the tilting of the BO_6 and $B'O_6$ octahedra to accommodate A cations having an appropriate (small enough) size (Woodward, 1997). The Glazer tilt system assigned to the space group $P2_1/n$ is 10, $a^-a^-b^+$ (Glazer, 1972, 1975). A more general approach, based on group-theoretical considerations, indicates that the monoclinic phase derives from the aristotype cubic phase *via* two distortions of comparable amplitude transforming according to the Γ^{4+} and X^{3+} irreducible representations of the space group $Fm\bar{3}m$ (Orobengoa *et al.*, 2009; Aroyo, Perez-Mato *et al.*, 2006). Hence the tilt system is physically described by means of symmetry-adapted modes (Faik *et al.*, 2009).

Evidence of monoclinic ($P2_1/n$) distortions of the unit cell has been observed in the diffraction patterns of Sr_2CaWO_6 at room temperature (Gateshki & Igartua, 2004). The temperature evolution of this structure reveals that the distortion of the unit cell becomes smaller at higher temperatures, almost disappearing at ~ 1100 K. Moreover, some peak intensities show very low values suggesting an I-centered lattice. At ~ 1130 K the diffraction pattern is consistent with a tetragonal body-centered unit cell and the space group $I4/m$. Finally, at ~ 1250 K, the tetragonal splitting of some diffraction lines disappears in a continuous way changing the structure from tetragonal ($I4/m$) to cubic ($Fm\bar{3}m$). Notice that although the space groups $I4/m$ and $P2_1/n$ share $Fm\bar{3}m$ as a common aristotype there is not a group–subgroup relationship between them. In accordance with previous results (Gateshki & Igartua, 2004), at room temperature Ca^{2+} and W^{6+} cations occupy the two crystallographically independent octahedral sites (Wyckoff positions 2*a* and 2*b*), while the Sr^{2+} cations occupy the 4*e* sites in a distorted environment defined by 12 O atoms which conform to the network of corner-sharing WO_6–CaO_6 octahedra.

The aim of this work is to present a simple and efficient route for preparing single crystals of double perovskite oxides of the Sr_2BWO_6 family as well as to show some intrinsic structural features derived from the high pseudosymmetry present in these materials. The samples have been structurally analyzed and compared with previous results obtained by powder diffraction methods.

2. Experimental

2.1. Sample preparation

Sr_2CaWO_6 was prepared by the co-precipitation method. Stoichiometric quantities of $Sr(NO_3)_2$ (I), $Ca(OOCH_3)_2$ (II) and $(NH_4)_{10}W_{12}O_{41}$ (III) were dissolved separately in distilled water. A slow addition, under magnetic stirring at room temperature, of (II) to a mixture of (I) and (III) induced the formation of a gelatinous precipitate. After evaporation at

Table 2
Summary of crystal data, experimental conditions and structure refinement details.

Notice that the same transformation matrix relates exactly the tetragonal and the cubic lattices.

Crystal data							
Chemical formula							Sr_2CaWO_6
M_r							247.6
Crystal system, space group							Irregular prism, $P2_1/n$
Temperature (K)							293
Lattice parameters	Data collection				Refinement		
a, b, c (Å)	8.207 (5), 8.208 (3), 8.216 (4)				5.800 (3), 5.813 (3), 8.207 (3)		
α, β, γ (°)	90.13 (5), 90.03 (6), 90.02 (6)				90.00 (5), 89.97 (5), 90.00 (5)		
V (Å^3)	553.4 (6)				276.7 (2)		
Crystal size (mm^3)					$0.12 \times 0.08 \times 0.05$		
Crystal colour					Light orange		
Approximate transformation matrix between the lattices	$(\mathbf{a}_m, \mathbf{b}_m, \mathbf{c}_m) \simeq (\mathbf{a}_c, \mathbf{b}_c, \mathbf{c}_c)\begin{pmatrix} 0 & 0 & -1 \\ \frac{1}{2} & \frac{1}{2} & 0 \\ \frac{1}{2} & -\frac{1}{2} & 0 \end{pmatrix}$						
Z							2
Density (Mg m^{-3}) X-rays							5.941
μ (mm^{-1})							40.83
Data collection							
Diffractometer							Stoe IPDS
Wavelength (Å)							0.71073
Detector distance (mm)							70
2θ range (°)							3.3/52.11
Number of exposures							150
Phi movement mode							Oscillation
Phi range (°)							0–300
Phi increment (°)							2
Profile function							Dynamic
Irradiation/exposure (min)							16
Smallest profile diameter (pixel)							9
Largest profile diameter (pixel)							29
Effective mosaic spread							0.020
Mean $F_o^2/\sigma(F_o^2)$							8.6
h, k, l	Data collection				Refinement		
	$-9 \rightarrow 10, -10 \rightarrow 10, -9 \rightarrow 9$				$-7 \rightarrow 7, -7 \rightarrow 7, -10 \rightarrow 10$		
Absorption correction							Analytical (Alcock, 1970)
Number of refined parameters							19
Refinement based on							F^2
Weighting scheme							$w = 1/[\sigma^2(F) + 0.045F^2]$
Extinction correction							None
Twin operations (see Table 4)		$R^+_{[001]}$	$R^-_{[001]}$	$R^+_{[110]}$	$R^-_{[110]}$	$R^+_{[1\bar{1}0]}$	$R^-_{[1\bar{1}0]}$
Refined twin fractions	0.20 (5)	0.03 (2)	0.06 (2)	0.16 (2)	0.18 (2)	0.24 (2)	0.13 (3)
$\Delta\rho_{max}, \Delta\rho_{min}$ (e Å^{-3})							2.33, −2.51
Refinement							
Unique reflections							566
Reflections with $[I>3\sigma(I)]$							350
R_{int} for 566 reflections averaged from 1910 intensities							9.62
$R_{obs}, R_{all}, wR_{all}, S_{obs}, S_{all}$							0.0420, 0.0681, 0.1339, 1.22, 1.03

Computer programs: *IPDS Software* (Stoe & Cie, 1998), *JANA*2000 (Petříček *et al.*, 2000), *CrystalMaker* (CrystalMaker Software Ltd, 2006).

333 K, the resulting powder was progressively heated in air at 473 K (12 h), 673 K (12 h), 873 K (12 h), 1173 K (24 h) and 1273 K (24 h). After each heating, the sample was cooled down slowly (3 K min^{-1}), and re-ground (re-mixed) to improve homogeneity. Phase purity was confirmed by X-ray powder diffraction. The synthesized Sr_2CaWO_6 powder was then used as the starting material for the single-crystal preparation. Single-crystal samples were obtained by sintering (Laudise, 1970) at 1953 K. Powder samples compressed (10 Ton for about 1 h) into dense rods were heated in platinum tubes up to 1953 K at a rate of 3 K min^{-1} in air atmosphere, held at this temperature for $\sim$ 48 h and then cooled to room temperature at a rate of 0.5 K min^{-1}. In this way an agglomerate of plate-like (up to 0.3×0.3 mm^2 in size) orange transparent crystals was obtained. Their quality and stoichiometry was confirmed by comparing the X-ray powder diagram of the obtained crystals with that of the starting material. No parasitic phases were found. Optical measurements show the presence of ferroelastic domains that could not be characterized owing to the unknown orientation and the small size of the samples that prevent an easy application of uniaxial stresses.

2.2. X-ray diffraction measurements

Conventional X-ray powder diffraction measurements at room temperature were carried out on a Philips X'Pert MPD system with Cu $K\alpha$ (Ni filter) radiation, equipped with a proportional detector. Intensity data were collected by continuous scanning with 2θ steps of 0.01° and counting times of 12 s at each step. The 2θ range covered was 15–120°. The Bragg–Brentano parafocusing geometry was used. Single crystals have been studied with a Stoe IPDS I, using monochromated Mo $K\alpha$ radiation. Details about the experimental conditions are given in Table 2.[2]

3. Symmetry considerations

The intensity distribution of the single-crystal data shows an almost cubic symmetry as shown in the reconstructed reciprocal sections of Fig. 1. A closer inspection of the reciprocal space indicates the existence of two separated diffraction patterns (with very different average intensities) whose mutual orientation made almost impossible any kind of Bragg peak superposition. Only the most intense diagram was considered. Intensities were indexed using a (pseudo)cubic cell, $a_c \simeq b_c \simeq c \simeq 8.21$ Å (see Table 2 and Fig. 1). Never-

[2] Supplementary data for this paper are available from the IUCr electronic archives (Reference: CK5040). Services for accessing these data are described at the back of the journal.

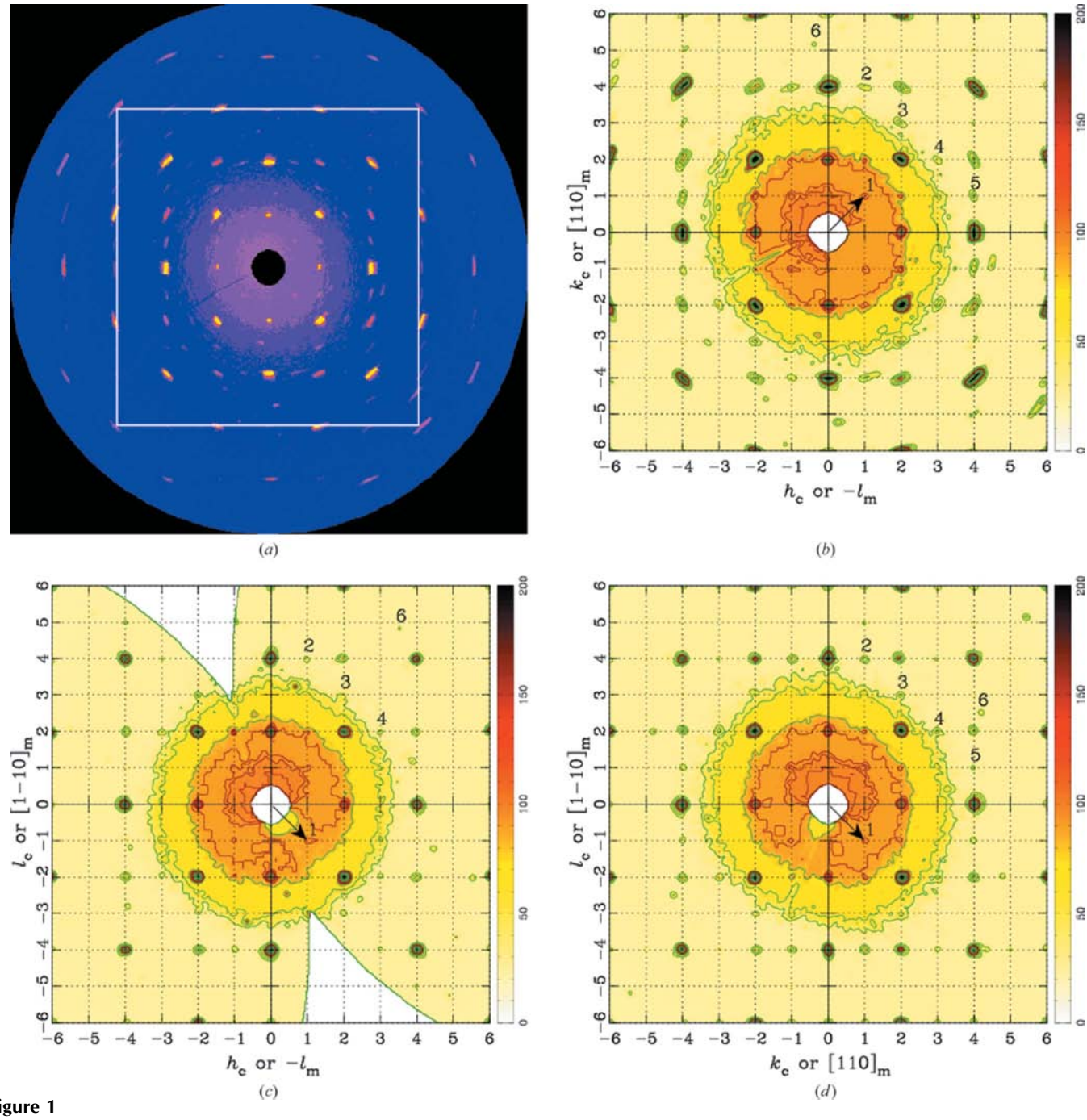

Figure 1
Reciprocal sections showing the high pseudosymmetry and the presence of twin domains in the diffraction pattern of Sr_2CaWO_6. (*a*) $(hk0)_c$ section reconstructed from the raw data. (*b*), (*c*) and (*d*) are contour plots extracted from the reciprocal planes $(hk0)_c$, $(h0l)_c$ and $(0kl)_c$. The range of Miller indices covers a squared region like the one sketched in (*a*). Reflections with all indices even belong to the cubic reciprocal lattice. Reflections lying outside the grid, like those marked with the number 6, belong to a small and misaligned specimen also present in the sample. The spots labelled by 1 and marked with arrows define the shortest axes of the monoclinic reciprocal cells. All marked spots break the *F* centering of the cubic phase. Some of them [case of 1, 3, 5 in (*b*); 1, 3 in (*c*); 2, 3, 4, 5 in (*d*) and in general those not having integer Miller indices in the reciprocal basis chosen for the refinement] belong to other twin domains as explained in Table 3. For example, the intensity of the spot labelled by 1 in the reciprocal plane $(hk0)_c$ is the sum of the intensities of the reflections (100) and (010) that belong to two different domains. Each of them is related to that chosen as the reference by rotation around the monoclinic direction [110] (*i.e.* the cubic axis $\mathbf{b}_c$) of 90 and -90°, respectively.

theless, previous powder diagrams at room temperature (Gateshki & Igartua, 2004) indicated a monoclinic structure with cell parameters a_m = 5.7672 (1), b_m = 5.8506 (1), c_m = 8.1931 (1) Å, β = 90.165 (1)° and consistent with the space group $P2_1/n$. When temperature is lowered this compound undergoes two consecutive phase transitions (Gateshki & Igartua, 2004) to a tetragonal structure (1250 K)[3]

[3] The cell transformations have been chosen in such a way that the refined atomic coordinates listed in Table 5 coincide with those published in Gateshki & Igartua (2004).

$[\mathbf{a}_t = 1/2(\mathbf{b}_c + \mathbf{c}_c), \mathbf{b}_t = 1/2(\mathbf{b}_c - \mathbf{c}_c), \mathbf{c}_t = -\mathbf{a}_c, I4/m]$ and to a monoclinic one (1130 K) ($\mathbf{a}_m \simeq \mathbf{a}_t$, $\mathbf{b}_m \simeq \mathbf{b}_t$, $\mathbf{c}_m \simeq \mathbf{c}_t$, $\beta \simeq 90^\circ$, $P2_1/n$). The space group of each phase is a subgroup of the cubic structure $Fm\bar{3}m$, but owing to the relative orientation of their symmetry elements there is no group–subgroup relationship between the tetragonal and the monoclinic phase. Given the group–subgroup indices of the space groups of the low-temperature phases into the cubic space group, the expected number of ferroelastic orientational states (related by the symmetry elements of the space group $Fm\bar{3}m$ not present in each subgroup) are as much as 6 and 12 for the tetragonal and monoclinic phases, respectively. In the case of the monoclinic structure most of the domain walls are determined by the components of the spontaneous strain tensor (Sapriel, 1975; *i.e.* they are not prominent planes with constant indices) and are temperature dependent. Only the six planes of the prototypic phase defined by the equations $x = 0$, $y = \pm z$, $y = 0$, $z = \pm x$, $z = 0$, $x = \pm y$ are strain-independent domain walls. To our knowledge only three attempts at twin volume refinement in the monoclinic double perovskites Pb_2CoWO_6 (Bonin *et al.*, 1995) and $A_2NaB'O_6$ (A = La, Pr, Nd and B' = Os, Ru; Gemmill, Smith & zur Loye, 2004; Gemmill *et al.*, 2005) have been reported. In the case of Pb_2CoWO_6 the twin operations correspond to symmetry elements (rotations of $\pm 90^\circ$ and 180° around one of the cubic axes) that belong to the space group of the parent phase. However, in the remaining cases the twin operation, selected without any explicit experimental or theoretical consideration, was a twofold rotation around the x axis and as a result of the refinement, the samples were considered untwinned. In the case of Sr_2CaWO_6 crystals the cubic symmetry of the diffraction patterns suggests the presence of twin domains related by fourfold rotations along the cubic axes or threefold rotations along the main diagonals of the cubic cell.[4] Although the reciprocal plane ($hk0$) shows some type of continuous arcs on each reciprocal lattice point they cannot be considered as a direct trace of twinning given their large spread when compared with the small deviation from 90° of the monoclinic angle. However, they could be due to small misorientations of the domain walls due to the lattice strain or, more probably, to misalignment of atomic layers during the crystal growth. The analysis of the systematic absences expected for the cubic space group shows that 381 measured reflections (of a total 3921) weakly violate the F-centering [only 4 reflections have a ratio $I/\sigma(I)>12$]. When the cubic cell is transformed into the monoclinic (or tetragonal) cell, about one half of the measured reflections (1964) can be indexed with integer Miller indices and 107 [only 1 satisfying $I/\sigma(I)>12$] do not fulfill the I-centering condition. Given the expected twin domains it is easy to test that the remaining measured reflections not belonging to the monoclinic reciprocal lattice have integer indices for the other (twin) orientation of the structure and also that those reflections that break the I-centering do not belong to any other possible twin domain where this centering is preserved (see Table 3). The data set fulfills the reflection conditions derived from the space group $P2_1/n$.

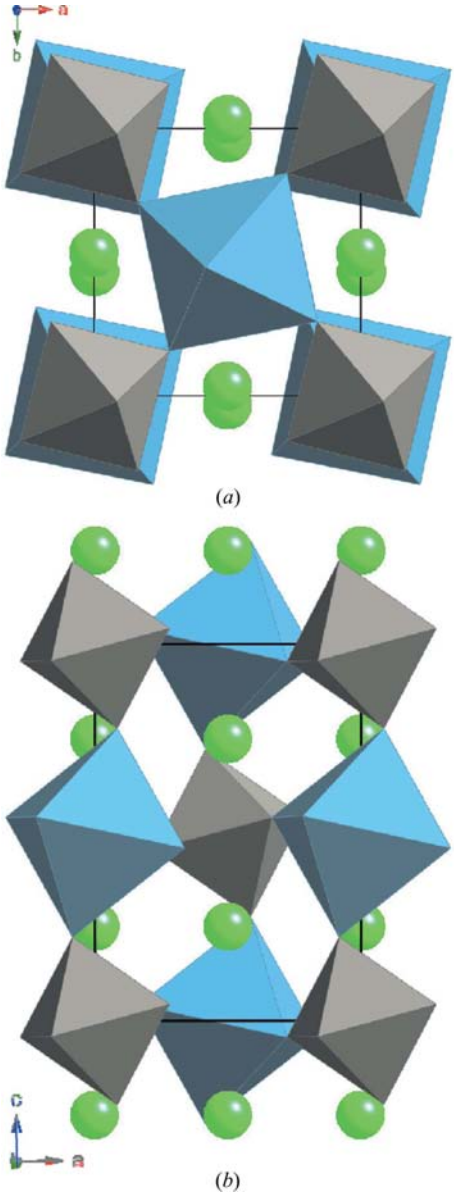

Figure 2
(*a*) (**a**,**b**) and (*b*) (**a**,**c**) projections of the structure of Sr_2CaWO_6. Grey and blue octahedra represent the W and Ca environments. Sr atoms are represented by isolated green balls.

4. Structure refinement

Keeping in mind the above considerations about the pseudosymmetry showed by the diffraction pattern, the structure can be straightforwardly refined as cubic ($Fm\bar{3}m$, R = 0.0339) and tetragonal ($I4/m$ with the change of basis indicated in Table 1, R = 0.0431). In the former case all the atomic coordinates are fixed except the x coordinate of the only independent O atom. In spite of the low R factor, the bond valences (Brown, 1996) calculated with *JANA*2000 (Petříček *et al.*, 2000) for W, Sr, Ca and O atoms were 5.87 (13),

[4] Given the number of possible ferroelastic orientational states the structural model includes the minimum number of parameters that explain the observed diffraction pattern (see Table 4).

Table 3
Indexing of the reflections marked in Fig. 1.

The transformations among the different twin domains are those of Table 4. The superscripts indicate the sense of rotation

				Miller indices in other twin domains					
Section	No.	'c' indices	'm' indices	$R^{+}_{[001]}$	$R^{-}_{[001]}$	$R^{+}_{[110]}$	$R^{-}_{[110]}$	$R^{+}_{[1\bar{1}0]}$	$R^{-}_{[1\bar{1}0]}$
$(hk0)_c$	1	(110)	$(\frac{1}{2}\frac{1}{2}\bar{1})$	–	–	(100)	(010)	–	–
	2	(140)	$(22\bar{1})$	$(2\bar{2}\bar{1})$	$(\bar{2}2\bar{1})$	–	–	–	–
	3	(230)	$(\frac{3}{2}\frac{3}{2}\bar{2})$	–	–	–	–	$(\bar{1}\bar{1}\bar{3})$	(113)
	4	(320)	$(11\bar{3})$	$(1\bar{1}\bar{3})$	$(\bar{1}1\bar{3})$	–	–	–	–
	5	(410)	$(\frac{1}{2}\frac{1}{2}\bar{4})$	–	–	–	–	$(\bar{2}\bar{2}\bar{1})$	(221)
$(h0\ell)_c$	1	$(10\bar{1})$	$(\frac{1}{2}\frac{1}{2}\bar{1})$	–	–	–	–	$(\bar{1}00)$	(010)
	2	(104)	$(2\bar{2}\bar{1})$	$(\bar{2}\bar{2}\bar{1})$	$(22\bar{1})$	–	–	–	–
	3	(203)	$(\frac{3}{2}\frac{3}{2}\bar{2})$	–	–	$(1\bar{1}3)$	$(\bar{1}1\bar{3})$	–	–
	4	(302)	$(1\bar{1}\bar{3})$	$(\bar{1}\bar{1}\bar{3})$	$(11\bar{3})$	–	–	–	–
$(0k\ell)_c$	1	$(01\bar{1})$	(010)	(100)	$(\bar{1}00)$	–	–	–	–
	2	(014)	$(\frac{5}{2}\frac{3}{2}0)$	–	–	–	–	$(2\bar{2}\bar{1})$	$(2\bar{2}1)$
	3	(023)	$(\frac{5}{2}\frac{1}{2}0)$	–	–	(113)	$(11\bar{3})$	–	–
	4	(032)	$(\frac{5}{2}\frac{1}{2}0)$	–	–	–	–	$(1\bar{1}\bar{3})$	$(1\bar{1}3)$
	5	(041)	$(\frac{5}{2}\frac{3}{2}0)$	–	–	(221)	$(22\bar{1})$	–	–

Table 4
Twin matrices [as defined in the program *JANA*2000 (Petříček *et al.*, 2000)] used during the refinement of the monoclinic phase of Sr_2CaWO_6.

A given reciprocal vector (h, k, l) is transformed as $(h, k, l)_o = (h, k, l)\mathbf{R}_{[o]}$, where $\mathbf{R}_{[o]}$ refers to the matrices that represent the symmetry elements of the space group $Fm\bar{3}m$ not present in the monoclinic structure, *i.e.* the transformations that relate the different monoclinic orientational states. Notice that the monoclinic directions [001], [110] and [1$\bar{1}$0] are the cubic axes $-\mathbf{a}_c$, $\mathbf{b}_c$ and $\mathbf{c}_c$ respectively.

$$R_{[001]}(90^\circ) = \begin{pmatrix} 0 & -1 & 0 \\ 1 & 0 & 0 \\ 0 & 0 & 1 \end{pmatrix} \qquad R_{[001]}(-90^\circ) = \begin{pmatrix} 0 & 1 & 0 \\ -1 & 0 & 0 \\ 0 & 0 & 1 \end{pmatrix}$$

$$R_{[110]}(90^\circ) = \begin{pmatrix} 1/2 & 1/ & 1 \\ 1/2 & 1/2 & -1 \\ -1/2 & 1/2 & 0 \end{pmatrix} \qquad R_{[110]}(-90^\circ) = \begin{pmatrix} 1/2 & 1/2 & -1 \\ 1/2 & 1/2 & 1 \\ 1/2 & -1/2 & 0 \end{pmatrix}$$

$$R_{[1\bar{1}0]}(90^\circ) = \begin{pmatrix} 1/2 & -1/2 & -1 \\ -1/2 & 1/2 & -1 \\ 1/2 & 1/2 & 0 \end{pmatrix} \qquad R_{[1\bar{1}0]}(-90^\circ) = \begin{pmatrix} 1/2 & -1/2 & 1 \\ -1/2 & 1/2 & 1 \\ -1/2 & -1/2 & 0 \end{pmatrix}$$

1.4284 (11), 3.00 (7) and 1.96 (6), indicating a deficient cation octahedral environment. In the case of the refinement in the tetragonal model the positions of the two independent O atoms were restricted through very tight W—O distances keeping the W bond valence as close as possible to its nominal value. The simplest structural model consistent with the observed diffraction pattern required three domains, two of which are related to the one whose coordinates are refined by positive fourfold rotations along $\mathbf{b}_c$ and $\mathbf{c}_c$. The strong absorption together with a high degree of pseudosymmetry introduces systematic errors that affect mainly the atomic displacement parameters (ADPs). As a consequence the atomic displacement parameters could not be refined as anisotropic. Moreover, the high difference in atomic number between the oxygen and the cations makes very difficult a reliable refinement of the ADP for O atoms. They were restricted to have the same value. In the last refinement cycles a rigid-body model for the WO_6 octahedron was used. Hence the tetragonal distortion can be described by a rotation of $-21.17\,(1)^\circ$ around the tetragonal axis ($\mathbf{a}_c$). The corner-sharing CaO_6 octahedra rotate correspondingly $17.23\,(1)^\circ$ around the same axis.

The monoclinic structure was also refined using a rigid-body model for WO_6 using a slightly distorted octahedron [1.90 (4) Å for the four equatorial W—O bonds and 1.92 (2) Å for the apical ones] that again (see below) restricts the atomic bond valences to values very close to their nominal values. The monoclinic distortion can then be described by two rotations (see Fig. 2) of 14.54 (1) and $-14.31\,(1)^\circ$ around the $\mathbf{c}_m$ ($[\bar{1}00]_c$) and $\mathbf{b}_m$ ($[01\bar{1}]_c$) axes, respectively.[5] The accompanying CaO_6 rotations are 11.707 (1) and $11.720\,(1)^\circ$. In this case the number of refined additional domains was 6 (see Tables 2 and 4), two of which appear in a lesser proportion. The atomic displacement parameters of O atoms were again restricted to have the same value and only the Sr displacement parameter could be refined as anisotropic, but forcing the off-diagonal terms of the tensor to null values. The final reliability factor ($R = 0.0420$)[6] was only slightly better than for the tetragonal model. The highest difference peak ($2.33\ e\ Å^{-3}$) and hole ($-2.51\ e\ Å^{-3}$) were located near O3 and O1 (and W), respectively. The calculated bond valences (Brown, 1996) for W, Ca, Sr and the three independent O atoms were 6.08 (16), 2.04 (6), 1.97 (6), 2.03 (11), 2.00 (6) and 2.01 (6). The eight O atoms that surround (up to 3 Å) each Sr atom define a coor-

[5] An almost identical model is obtained considering a twinning model where the different domains are related by (positive and negative) threefold cubic rotations

[6] Untwinned models give R factors of 0.0597 and 0.0591 for the tetragonal and monoclinic models.

Table 5
Final values for the positional and atomic displacement parameters.

The coordinates of the independent octahedron fragment [W—O1—O2—O3] were refined as belonging to a rigid body which is tilted around the monoclinic axes, $R_a = -0.333$ (6), $R_b = -14.31$ (1) and $R_c = 14.54$ (1)°, with respect to the corresponding octahedron in the cubic phase. The standard uncertainties of the O atoms have been estimated by an additional cycle of refinement without restrictions. The off-diagonal components of the Sr displacement tensor were fixed to zero (see text).

	x	y	z	U^{11}/U_{iso}	U^{22}	U^{33}
W	0	0	0	0.0027 (4)	–	–
Ca	0	0	1/2	0.0053 (11)	–	–
Sr	0.0010 (19)	0.5358 (10)	0.2502 (10)	0.013 (3)	0.012 (2)	0.001 (3)
O1	0.079 (5)	0.018 (4)	−0.224 (5)	0.038 (4)	–	–
O2	0.277 (3)	−0.169 (4)	0.042 (3)	0.038 (4)	–	–
O3	0.161 (4)	0.283 (3)	0.040 (3)	0.038 (4)	–	–

Table 6
Most relevant distances (Å) and angles (°) concerning the constrained octahedral environments of W and Ca atoms.

The uncertainties have been estimated using the coordinates (and the corresponding standard deviations) given in Table 5.

W—O1	1.90 (4)	O1—W—O2	90.0 (11)	O1—W—O3	90.0 (11)
W—O2	1.92 (2)	O2—W—O3	90.1 (10)		
W—O3	1.917 (18)				
Ca—O1^{i}	2.31 (4)	O1^{i}—Ca—O2^{ii}	90.2 (9)	O1^{i}—Ca—O3^{iii}	90.3 (10)
Ca—O2^{ii}	2.34 (2)	O2^{ii}—Ca—O3^{iii}	87.6 (7)		
Ca—O3^{iii}	2.36 (2)				

Symmetry codes: (i) $x, y, 1+z$; (ii) $-\frac{1}{2}+x, -\frac{1}{2}-y, \frac{1}{2}+z$; (iii) $-\frac{1}{2}+x, \frac{1}{2}-y, \frac{1}{2}+z$.

dination polyhedron of 30.5 Å^3 (Koch & Fischer, 1996). Final atomic parameters and bond distances are shown in Tables 5 and 6.

5. Concluding remarks

Sintering at high temperature has been shown to be a new and efficient method for growing single crystals of double perovskites suitable not only for X-ray diffraction but also for a better analysis of optical, electrical or magnetic properties. However, structural analysis of these materials requires special attention. The combined effects of absorption, pseudosymmetry and twinning may mask subtle but important details. The particular case of Sr_2CaWO_6 exemplifies many of the inherent difficulties in structure determinations of this kind of compound. It has been shown how a blind refinement in the space groups $Fm\bar{3}m$ gives satisfactory results. More elaborate models of lower symmetry require a full and rigorous consideration of the possible orientational states and therefore a group-theoretical study of the phase transition. In the present case both low-temperature space groups are subgroups of the parent group, but there is no group–subgroup relation between the space groups $I4/m$ and $P2_1/n$ given the mutual orientation of their symmetry elements. In each phase the different domains are related by the symmetry elements of the common parent phase lost in the phase transition. This preliminary work, that can be done straightforwardly using for example the Bilbao Crystallographic Server (Aroyo, Kirov *et al.*, 2006), would prevent some attempts of refining twinning laws that could be inconsistent with the observed diffraction patterns (Gemmill, Smith & zur Loye, 2004; Gemmill *et al.*, 2005).

This work has been supported by the projects MAT2008-05839/MAT and IT-282-07.

References

Alcock, N. W. (1970). *Crystallographic Computing*, edited by F. R. Ahmed, S. R. Hall & C. P. Huber, pp. 271–278. Copenhagen: Munksgaard.

Aroyo, M. I., Kirov, A., Capillas, C., Perez-Mato, J. M. & Wondratschek, H. (2006). *Acta Cryst.* A**62**, 115–128.

Aroyo, M. I., Perez-Mato, J. M., Capillas, C., Kroumova, E., Ivantchev, S., Madariaga, G., Kirov, A. & Wondratschek, H. (2006). *Z. Kristallogr.* **221**, 15–27.

Bharathy, M. & zur Loye, H.-C. (2008). *J. Solid State Chem.* **181**, 2789–2795.

Bonin, M., Paciorek, W., Schenk, K. J. & Chapuis, G. (1995). *Acta Cryst.* B**51**, 48–54.

Brown, I. D. (1996). *J. Appl. Cryst.* **29**, 479–480.

Chmaissem, O., Kruk, R., Dabrowski, B., Brown, D. E., Xiong, X., Kolesnik, S., Jorgensen, J. D. & Kimball, C. W. (2000). *Phys. Rev. B*, **62**, 14197–14206.

CrystalMaker Software Ltd (2006). *CrystalMaker.* CrystalMaker Software Ltd, Bicester, Oxfordshire, England.

Davis, M. J., Mugavero III, S. J., Glab, K. I., Smith, M. D. & zur Loye, H.-C. (2004). *Solid State Sci.* **6**, 413–417.

DeMarco, M., Blackstead, H. A., Dow, J. D., Wu, M. K., Chen, D. Y., Chien, F. Z., Haka, M., Toorongian, S. & Fridmann, J. (2000). *Phys. Rev. B*, **62**, 14301–14303.

Faik, A., Igartua, J. M., Gateskhi, M. & Cuello, G. J. (2009). *J. Solid State Chem.* **182**, 1717–1725.

Gateshki, M. & Igartua, J. M. (2004). *J. Phys. Condens. Matter*, **16**, 6639–6649.

Gemmill, W. R., Smith, M. D. & zur Loye, H.-C. (2004). *J. Solid State Chem.* **177**, 3560–3567.

Gemmill, W. R., Smith, M. D., Prozorov, R. & zur Loye, H.-C. (2005). *Inorg Chem.* **44**, 2639–2646.

Glazer, A. M. (1972). *Acta Cryst.* B**28**, 3384–3392.

Glazer, A. M. (1975). *Acta Cryst.* A**31**, 756–762.

Kobayashi, K.-I., Kimura, T., Sawada, H., Terakura, K. & Tokura, Y. (1998). *Nature*, **395**, 677–680.

Koch, E. & Fischer, W. (1996). *Z. Kristallogr.* **211**, 251–253.

Laudise, R. A. (1970). *The Growth of Single Crystals.* New Jersey: Prentice-Hall Inc.

Martin, L. O., Chapman, J. P., Hernández-Bocanegra, E., Insausti, M., Arriortua, M. I. & Rojo, T. (2004). *J. Phys. Condens. Matter*, **16**, 3879–3888.

Mitchell, R. H. (2001). *Perovskites. Modern and Ancient*. Almaz Press.

Mugavero, S. J., Smith, M. D. & zur Loye, H.-C. (2005). *J. Solid State Chem.* **178**, 200–206.

Mugavero III, S. J., Puzdrjakova, I. V., Smith, M. D. & zur Loye, H.-C. (2003). *Acta Cryst.* E**61**, i3–i5.

Orobengoa, D., Capillas, C., Aroyo, M. I. & Perez-Mato, J. M. (2009). *J. Appl. Cryst.* **42**, 820–833.

Petříček, V., Dušek, M. & Palatinus, L. (2000). *JANA*2000. Institute of Physics, Prague, Czech Republic.

Roof, I. P., Smith, M. D. & zur Loye, H.-C. (2008). *J. Cryst. Growth*, **310**, 240–244.
Sapriel, J. (1975). *Phys. Rev. B*, **12**, 5128–5140.
Stitzer, K. E., Smith, M. D. & zur Loye, H.-C. (2002). *Solid State Sci.* **4**, 311–316.
Stoe & Cie (1998). *IPDS Software*, Version 2.87. Stoe and Cie GmbH, Darmstadt, Germany.
Woodward, P. M. (1997). *Acta Cryst.* B**53**, 32–43.
Yamamura, K., Wakeshima, M. & Hinatsu, Y. (2006). *J. Solid State Chem.* **179**, 605–612.